



FERMILAB-Pub-80/82-THY
September 1980

Avoidance of Counter-Example to Non-Abelian Bloch-Nordsieck Conjecture by Using Coherent State Approach

C.A. NELSON*

Fermi National Accelerator Laboratory, Batavia, Illinois 60510

ABSTRACT

It is shown that the counter-example to non-Abelian Bloch-Nordsieck conjecture in " $q + \bar{q} \rightarrow \gamma^* + \text{soft gluons}$ " to order α_s^2 is avoided at the cross section level if the initial-state is prepared according to the coherent state approach for treatment of the infrared region of non-Abelian gauge theories.

*Permanent address: Department of Physics, State University of New York at Binghamton, Binghamton, New York 13901.

I. INTRODUCTION

In a recent paper Doria, Frenkel and Taylor¹ have discussed a counter-example to the non-Abelian Bloch-Nordsieck² conjecture that if both final-state real soft gluons and virtual soft gluons are summed, the IR divergences will cancel in the (color averaged) cross section in perturbative QCD. In later papers³ they and their collaborators have constructed and analyzed the simpler counter-example which is considered here. These counter-examples[†] have prompted questions concerning the validity of arguments for the factorization and universality of mass singularities in hard scattering processes for the latter arguments assumed no length cutoff, for example associated with the spatial extent of a hadron, is necessary to insure cancellation of IR divergences.

The purpose of this paper is to show that the simple α_s^2 counter-example "q + $\bar{q} \rightarrow \gamma^* + \text{soft gluons}$ ", with γ^* a hard virtual photon, is avoided at the cross section level if the initial-state is prepared according to the coherent state constructive procedure for the non-Abelian case. This is a perturbative procedure and has been developed^{7,8} in analogy with that used^{9,10} in the Abelian case. In our calculation we adopt the notation and approach, and only extend the analysis of Sec. 2 of Andradi, *et al.*³ by including the corresponding IR contributions from the initial-states' part which then gives an IR finite cross section.

For completeness and to emphasize the assumptions, in Sec. II the coherent state approach is reviewed. Diagram rules needed in the present calculation to construct the initial-state contributions are listed in an appendix. In Sec. III the IR divergences arising from virtual soft gluons in the usual covariant graph are shown to be cancelled in the cross section by contributions from the initial-state. This

[†] Such counter-examples can be shown not to occur for many processes using the methods of Libby and Sterman [Ref. 5] and the present counter-example has been considered [Ref. 3] relative to the Kinoshita-Lee-Nauenberg Theorem [Ref. 6]. Much of reference 1 has been checked in reference 4.

occurs separately for each topological type of covariant graph. Similarly, in Sec. IV, the IR divergences arising from final real soft-gluon emission are shown to be cancelled in the cross section by contributions from the initial-state.

II. REVIEW

The coherent state treatment of the asymptotic dynamics in the infrared region of non-Abelian gauge theory is an amplitude approach in perturbation theory which is based on the asymptotic behavior of the Hamiltonian operator for $|t| \rightarrow \infty$ in the interaction representation. As in the treatment of scattering in an unscreened Coulomb potential in quantum mechanics and in the coherent state treatment^{9,10} of the IR region in QED and gravitation, the motivating idea is to avoid the IR divergences by rewriting the total Hamiltonian

$$\begin{aligned} H &= H_0 + H_I \\ &= H_{as} + H'_I \end{aligned} \tag{1}$$

where $H_{as}(t) = H_0 + V_{as}(t)$ so that H'_I does vanish sufficiently fast asymptotically to avoid IR divergences. Since the quark mass is chosen to be finite, the asymptotic Hamiltonian $H_{as}(t)$ does not contain $q\bar{q}$ creation or annihilation pieces. It does include the complete cubic and quartic gluon self-coupling terms. The associated time evolution operator, $U_{as}(t)$, in Schrödinger representation

$$\frac{idU_{as}(t)}{dt} = H_{as}(t)U_{as}(t) \tag{2}$$

is then used to generate an initial asymptotic states' space $\mathcal{H}_{as} = \exp[-\Omega(t)] \mathcal{H}_F$, where $t \rightarrow -\infty$, from the usual Fock space \mathcal{H}_F . Because of the presence of massless gauge quanta, \mathcal{H}_{as} is not the free particle basis based on H_0 .

Being asymptotic in origin, the construction of \mathcal{H}_{as} based on Eq. (1) is not unique. More significantly, because of the conjectured confinement property for QCD which forbids all systems with color-nonsinglet quantum numbers from existing as isolated objects, and because of the apparent empirical absence of Van der Waals forces, it is not yet clear how physical are the properties of the non-Abelian perturbative IR region.^{††} Unfortunately, we have to "with-hold judgment" on this issue for the present analysis will not incorporate such important nonperturbative long-range effects since we do not know if they are sufficiently well understood at present to be included. A somewhat similar assumption is necessary in Stermann-Weinberg inclusive cross-section analyses. Nevertheless, just as the Coulomb phase shift is observable in well-chosen reactions, the IR domain in QCD may eventually turn out to be physical despite the presence of nonperturbative effects.

The perturbative solution of Eq. (2) for the asymptotic time evolution operator, $U_{as}(t)$, can be written as in the usual coherent state operator exponentiation (Magnus' Theorem)

$$U_{as}(t) = \exp(-i H_0 t) Z(t) \quad (3)$$

$$Z(t) = \exp[\Omega(t)] \quad , \quad \Omega^\dagger(t) = -\Omega(t) \quad (4)$$

^{††} We thank Bill Bardeen for emphasizing this point.

where $\Omega(t)$ is given by iterative integrations over an infinite series of Lie elements of the asymptotic potential, $V_{as}(t)$. Equivalently, Eq. (2) can be solved as in time-ordered perturbation theory

$$Z(t) = 1 + \sum_{n=1}^{\infty} (-i)^n \int^t dt_1 \int^{t_1} dt_2 \dots \int^{t_{n-1}} dt_n V_{as}(t_1) \dots V_{as}(t_n) \quad (5)$$

and used to generate the equally-weighted diagrams shown in Figs. 1-5 via the definitions ($|\psi_F\rangle$ is in interaction representation)

$$|\psi_{as}\rangle = \lim_{t \rightarrow -\infty} \{ Z^\dagger(t) \} |\psi_F\rangle \quad (6)$$

$$S^G(t_1, t_2) = \lim_{\substack{t_1 \rightarrow \infty \\ t_2 \rightarrow -\infty}} Z^\dagger(t_1) S_D(t_1, t_2) Z(t_2) \quad (7)$$

Order by order, $Z(t)$ can be expressed in terms of $\Omega(t)$.

Even in the Abelian case⁹ this is a formal (heuristic) procedure because $Z(t)$, when precisely defined, turns out not to be a unitary operator in \mathcal{H}_F ; in fact, $|\psi_{as}\rangle$ are representations of the canonical commutation rules which are unitarily inequivalent to the Fock representation. To specify $Z(t)$, Eqs. (5)-(7), require "boundary conditions." Since the idea is to modify H_0 to H_{as} only at large $|t|$, in Eq. (5) contributions of the lower end point of integration are dropped* (in the Abelian case this assumption is necessary for $\Omega(t)$ to commute asymptotically with the total momentum operator)⁹. Note that H_I is used in calculating the usual Dyson S operator, S_D in Eq. (7). Also in the Abelian case, in Eq. (4), the $\Omega(t)$

* In Eq. (7) the endpoint for $Z(t_2)$, and for specifying initial-states' space, could be chosen as $(t_2)_0 = -\infty$ and for $Z(t_1)$, and for final states' space, as $(t_1)_0 = +\infty$ with the assumption of an $\pm i\epsilon$ prescription to avoid endpoint contributions. An ϵ has been displayed explicitly in the present calculation. If ϵ is equal to zero (this was done in Ref. 9 in showing the cancellation in the matrix element of the IR divergent $\Phi(t)$ contributions to the scattering operator defined by Eq. 7), the IR divergences in the cross section still cancel separately for each topological set.

perturbative series of integrations over Lie elements truncates and $\Omega(t) = R(t) + i\Phi(t)$. It is found that in Eq. (7), $R(t) \rightarrow 0$ as $|t| \rightarrow \infty$, but $\Phi(t)$ is odd asymptotically and, when regularized, cancels the IR divergent Coulomb phase. In the present paper on the non-Abelian case we do not consider non-trivial generalizations of Φ type of terms (c.f. Ref. 8) so we only treat the cancellation of the IR divergences in the cross section. However, it is easy to show that the $R(t)$ type terms associated with Figures 1-5 vanish in Eq. (7) as $t_2 \rightarrow -\infty$.

For $R(t)$ terms in Eq. (6) in the non-Abelian case we adopt as a working "ansatz" the replacement in quark Bremsstrahlung terms of

$$a_{a\mu}^\dagger(k) e^{i \frac{k \cdot p}{p_0} t} \rightarrow a_{a\mu}^\dagger(k) = \sum_m e_\mu^{(m)} a_i^\dagger \quad (8)$$

where $e_\mu^{(m)}(k)$ are gluon polarization vectors with $i = (a, m, \vec{k})$ denoting "a" for the color gauge-group index, "m" for the spin polarization, and " \vec{k} " for the on-mass shell gluon three-momentum. Similarly, for other terms of Eq. (5) in n-th order, we assume

$$(\text{operators}) e^{i[E_0 - E_n] t} \rightarrow (\text{operators}) \quad (9)$$

so $Z^\dagger(t) \rightarrow Z^\dagger$ and Eq. (6) becomes the time-independent relation

$$|\psi_{as}\rangle = Z^\dagger |\psi_F\rangle \quad (10)$$

Again, in the Abelian case by working in the complete infinite tensor product space of von Neumann, Eq. (8) has been justified and \mathcal{H}_{as} , defined by Eq. (6), has been

shown to be t independent and to contain a Lorentz and gauge invariant subspace with nonnegative metric.⁹

Accepting this constructive procedure, graphical rules for $|\psi_{as}\rangle$ are easy to derive and the ones needed for the calculation to order α_s^2 for " $q + \bar{q} \rightarrow \gamma^* + \text{soft gluons}$ ", with γ^* a hard virtual photon, are listed in the appendix. In this approach it is not necessary, in order to cancel IR divergences in the cross section, to sum over final color spins and to average over initial color spins since each asymptotic color-charged particle, e.g. quark or gluon, is accompanied by its associated color-singlet set of self-interacting soft gluons.⁸

III. CANCELLATION OF VIRTUAL GLUON IR DIVERGENCES

As discussed by Andradi, et al.³ the α_s^2 color and spin averaged cross section for " $q + \bar{q} \rightarrow \gamma^* + \text{soft gluons}$ " has the form

$$\alpha_s^2 \sigma_B \left\{ A C_F^2 + N C_F C_{YM} \right\} \quad (11)$$

where σ_B is the Born cross section and, with t_a the Hermitian representation matrices for quarks,

$$t_a t_a = C_F 1, \quad f_{abc} f_{abd} = C_{YM} \delta_{cd}$$

where $[t_a, t_b] = i f_{abc} t_c$ [$C_{YM} = 0$ in Abelian case]. Following these authors, we work in the lab frame of the anti-quark $p^\mu = (m; \vec{0})$, use the Coulomb Gauge defined in this frame, and make the eikonal approximation in the contribution from the graph part. The graphs contributing to N and responsible for the counter-example

to the non-Abelian Bloch-Nordsieck conjecture are labeled with "0" in Figs. 1-5. For the cross section, the amplitude for each virtual topological set [a, b, c, d in Figs. 1-4] is to be multiplied by the complex conjugate of the Born amplitude, and then the complex conjugate of this product is to be added, followed by the color and spin averaging. Notation used in the figures is explained in the caption to Fig. 1. Note that on-shell particles bridge the initial-state, graph, and final-state parts so usage of the Coulomb Gauge reduces significantly the number of diagrams associated with contributions from the initial-states' parts. We do not consider here the graphs in which gluons are attached solely to the quark, or to the anti-quark line, for such graphs are not responsible for the counter-example.

In the coherent state approach, cancellation of IR divergences has been found to occur separately in each topological set. The first such set, (a), is shown in Fig. 1. With \mathcal{M}_B the Born amplitude, we remove some factors common to each graph in Fig. 1 by writing

$$\mathcal{M}_{ai} = -\mathcal{M}_B t_b t_a t_b t_a \frac{g^4}{(2\pi)^6} \bar{\mathcal{M}}_{ai} \quad ; \quad i = 0, \dots, 3 \quad (12)$$

As in Andrasi, et al.³ Fig. (a0) gives

$$\begin{aligned} \bar{\mathcal{M}}_{a0} = & -\frac{1}{2}\beta^2 \int d^3k d^3L [1 - x^2] k^{-1} L^{-2} [k - K]^{-1} [L + i\epsilon]^{-1} \\ & \times [-k + K + L + i\epsilon]^{-1} \quad , \end{aligned} \quad (13)$$

where

$$k = |\vec{k}| \quad , \quad K = \vec{k} \cdot \vec{q} / q_0 = \beta kx, \dots \quad (14)$$

and Fig. (a1) gives

$$\begin{aligned}
 \overline{\mathcal{M}}_{a1} &= i(2\pi)^{-1} \frac{1}{2} \beta^2 \int d^3k d^4\ell [1 - x^2] k^{-1} \ell^{-2} [\ell_0 + i\epsilon]^{-1} \\
 &\quad \times [-\ell_0 + k + L - K + i\epsilon]^{-1} [-\ell_0 + L + i\epsilon]^{-1} [k - K]^{-1} \\
 &= -\overline{\mathcal{M}}_{a0} .
 \end{aligned} \tag{15}$$

For (a1) in applying graphical rules, one must include factor $(e_v^{(\ell)}(k)/[2(2\pi)^3 k_0]^{1/2})u(q)$ for joining graph and initial-state and also sum over (a, ℓ, \vec{k}) gluon indices. Since k is an on-mass-shell gluon, the quark momentum following Coulomb gluon, $\vec{\ell}$, emission is $(q_1)_\mu \simeq (q - \ell)_\mu$ and then following \vec{k} absorption it is $(q_2)_\mu \simeq (q - \ell + k)_\mu$. Similarly, for Fig. (a2) following \vec{k} absorption $(q_1)_\mu \simeq (q + k)_\mu$ so we obtain

$$\overline{\mathcal{M}}_{a2} = -\overline{\mathcal{M}}_{a0} (\epsilon \rightarrow \bar{\epsilon}) \tag{16}$$

(note minus sign from anti-quark incident) and for Fig. (a3)

$$\begin{aligned}
 \overline{\mathcal{M}}_{a3} &= -\frac{1}{2} \beta^2 \int d^3k d^3\ell [1 - x^2] k^{-1} \ell^{-2} [k - K]^{-1} \\
 &\quad \times [L - i\bar{\epsilon}]^{-1} [-k + K + L - i\bar{\epsilon}]^{-1}
 \end{aligned} \tag{17}$$

so

$$\text{Re} [\overline{\mathcal{M}}_{a3}] = -\text{Re} [\overline{\mathcal{M}}_{a2}] . \tag{18}$$

For topological set (b), we let

$$\mathcal{M}_{bi} = -i \mathcal{M}_B^t t_c^t t_b^t t_a^f f_{abc} \frac{g^4}{(2\pi)^6} \bar{\mathcal{M}}_{bi} \quad ; \quad i = 0, 1, 2 \quad . \quad (19)$$

For Fig. (b0), do the s_0 -integration by closing in the lower half-plane and then k_0 by also closing in lower half-plane so

$$\begin{aligned} \mathcal{M}_{b0} = & \beta \int d^3k d^3s [y - x \cos \psi] s^{-1} k^{-1} [(\vec{s} + \vec{k})^2]^{-1} \\ & \times [k - K]^{-1} [K + S + i\epsilon]^{-1} \end{aligned} \quad (20)$$

with

$$\vec{k} \cdot \vec{s} = ks \cos \psi \quad , \quad S = \vec{s} \cdot \vec{q} / q_0 = \beta sy \quad .$$

Similar to set (a) calculations,

$$\begin{aligned} \bar{\mathcal{M}}_{b1} = & -\beta \int d^3k d^3s [y - x \cos \psi] s^{-1} k^{-1} [(\vec{s} + \vec{k})^2]^{-1} \\ & \times [k - K]^{-1} [k + S + i\epsilon]^{-1} \end{aligned} \quad (21)$$

and

$$\begin{aligned} \bar{\mathcal{M}}_{b2} = & -\beta \int d^3k d^3s [y - x \cos \psi] s^{-1} k^{-1} [(\vec{s} + \vec{k})^2]^{-1} \\ & \times [K + S + i\bar{\epsilon}]^{-1} [k + S + i\bar{\epsilon}]^{-1} \end{aligned} \quad (22)$$

so

$$\text{Re}[\overline{\mathcal{M}}_{b0} + \overline{\mathcal{M}}_{b1} + \overline{\mathcal{M}}_{b2}] = 0 \quad . \quad (23)$$

For topological set (c), let

$$\mathcal{M}_{ci} = -i\mathcal{M}_B^t t_b^t t_a^t f_{abc} \frac{g^4}{(2\pi)^6} \overline{\mathcal{M}}_{ci} \quad ; \quad i = 0,1,2 \quad (24)$$

so

$$\begin{aligned} \overline{\mathcal{M}}_{c0} &= -\beta \int d^3k d^3s [y - x \cos \psi] s^{-1} k^{-1} [(\overrightarrow{s+k})^2]^{-1} \\ &\times [K + S + i\epsilon]^{-1} [k + S - i\epsilon]^{-1} \quad . \end{aligned} \quad (25)$$

For (c1), following absorption of s' gluon, $(q_1)_\mu \simeq (q + s')_\mu$ so

$$\begin{aligned} \overline{\mathcal{M}}_{c1} &= -\beta \int d^3k d^3s [y - x \cos \psi] s^{-1} k^{-1} [(\overrightarrow{s+k})^2]^{-1} \\ &\times [k - K]^{-1} [k + S - i\bar{\epsilon}]^{-1} \end{aligned} \quad (26)$$

and for (c2)

$$\begin{aligned} \mathcal{M}_{c2} &= \beta \int d^3k d^3s [y - x \cos \psi] s^{-1} k^{-1} [(\overrightarrow{s+k})^2]^{-1} \\ &\times [k - K]^{-1} [K + S - i\bar{\epsilon}]^{-1} \end{aligned} \quad (27)$$

so

$$\text{Re} [\overline{\mathcal{M}}_{c0} + \overline{\mathcal{M}}_{c1} + \overline{\mathcal{M}}_{c2}] = 0 \quad . \quad (28)$$

Topological set (d) is more complicated for there are 3 energy-orderings of the vertices. In Ref. 8, for simple tree graphs it was found that the IR cancellation occurs not only for distinct topological sets of each covariant graph, but actually at level of each energy-ordered subset of the topological set. Set (d), however, is sufficiently simple to directly do standard contour integration of the amplitudes associated with the graph part. Letting

$$\mathcal{M}_{di} = i \mathcal{M}_{B^t C^t b^t a^f cba} \frac{g^4}{(2\pi)^6} \overline{\mathcal{M}}_{di} \quad ; \quad i = 0, \dots, 5 \quad (29)$$

for (d0), following Andradi, et al.³ we obtain

$$\begin{aligned} \overline{\mathcal{M}}_{d0A} = & - \int d\mu [k + s]^{-1} [K + S + i\epsilon]^{-1} \\ & \times [s - K - i\epsilon]^{-1} [k - K]^{-1} \end{aligned} \quad (30)$$

where convenient measure is [it is invariant under $\vec{k} \rightarrow -\vec{k}$, $\vec{s} \rightarrow -\vec{s}$, as well as under $\vec{k} \leftrightarrow \vec{s}$]

$$\begin{aligned} \int d\mu = & \beta^2 \int d^3k d^3s [1 - x^2 - y^2 + xy \cos \psi] [(\vec{k} + \vec{s})^2]^{-1} \\ \vec{k} \cdot \vec{s} = & ks \cos \psi \end{aligned} \quad (31)$$

and from two gluon-propagator poles obtain

$$\begin{aligned} \overline{\mathcal{M}}_{d0B} = & \frac{1}{4} \int d\mu (s-k) k^{-1} s^{-1} [k+s]^{-1} [k-K]^{-1} \\ & \times [k+s-K-S]^{-1} . \end{aligned} \quad (32)$$

For (d1) do s_0 -integration by closing contour in lower half-plane. Residue from graph parts' gluon-propagator pole vanishes for asymmetric under $s_\mu \leftrightarrow k_\mu$, so obtain

$$\begin{aligned} \overline{\mathcal{M}}_{d1} = & - \int d\mu [k+s]^{-1} [k-s+i\epsilon]^{-1} [k-K]^{-1} \\ & \times [k+S+i\epsilon]^{-1} . \end{aligned} \quad (33)$$

We can show

$$\text{Re} [\overline{\mathcal{M}}_{d0A} + \overline{\mathcal{M}}_{d1}] = 0 \quad (34)$$

by adding complex conjugate amplitude with change of variables $\vec{s} \rightarrow -\vec{s}$, $\vec{k} \rightarrow -\vec{k}$ and then relabeling $s_\mu \leftrightarrow k_\mu$. For (d2), factor for joining graph and initial-state is

$$\frac{1}{2} \left(\frac{e_v^{(m)}(s)}{[2(2\pi)^3 s_0]^{1/2}} \right) \left(\frac{e_\mu^{(l)}(k)}{[2(2\pi)^3 k_0]^{1/2}} \right) u(q)$$

and contract two incident gluons in both ways for state; obtain

$$\overline{\mathcal{M}}_{d2} = - \overline{\mathcal{M}}_{d0B} \quad (35)$$

so, up to this point there are no net IR divergences for set (d).

For (d3) we obtain

$$\begin{aligned} \overline{\mathcal{M}}_{d3} = & -\frac{1}{4} \int d\mu(s-k) k^{-1} s^{-1} [k+s]^{-1} [k-K]^{-1} \\ & \times [k+s-K-S]^{-1} . \end{aligned} \quad (36)$$

For (d4) there are two energy-orderings for state, in case $k_0 < 0$ (k_μ shown in Fig. 4, do) so gluon \vec{k}' absorbed by quark,

$$\begin{aligned} \overline{\mathcal{M}}_{d4A} = & \frac{1}{4} \int d\mu(s-k) s^{-1} k^{-1} [k-K]^{-1} [s-S]^{-1} \\ & \times [s+K-i\bar{\epsilon}]^{-1} \end{aligned} \quad (37)$$

and for case $k_0 > 0$, i.e. \vec{k} emitted,

$$\begin{aligned} \overline{\mathcal{M}}_{d4B} = & \frac{1}{4} \int d\mu(s+k) s^{-1} k^{-1} [k-s+i\bar{\epsilon}]^{-1} [s-K-i\bar{\epsilon}]^{-1} \\ & \times [s+S]^{-1} . \end{aligned} \quad (38)$$

The $i\epsilon$ in $[k-s+i\epsilon]^{-1}$ in $\overline{\mathcal{M}}_{d4B}$ and in $\overline{\mathcal{M}}_{d1}$ are unimportant since the terms multiplying $[k-s+i\epsilon]^{-1}$ vanish when $k=s$. Fig. (d5) has 3 energy-orderings for state part, case $s'_0 > 0$, $k_0 > 0$ gives

$$\begin{aligned} \overline{\mathcal{M}}_{d5A} = & \frac{1}{4} \int d\mu(s+k) s^{-1} k^{-1} [K+S+i\bar{\epsilon}]^{-1} \\ & \times [k+S+i\bar{\epsilon}]^{-1} [s+S]^{-1} . \end{aligned} \quad (39)$$

As for Eq. (34), we can show

$$\text{Re} [\mathcal{M}_{d4B} + \mathcal{M}_{d5A}] = 0 \quad . \quad (40)$$

In case, $s'_0 < 0$, $k_0 > 0$, Fig. (d5) gives

$$\begin{aligned} \mathcal{M}_{d5B} &= -\frac{1}{4} \int d\mu (s-k) s^{-1} k^{-1} [k+s]^{-1} [K+S+i\tilde{\epsilon}]^{-1} \\ &\quad \times [k+S+i\tilde{\epsilon}]^{-1} \end{aligned} \quad (41)$$

and for $s'_0 > 0$, $k_0 < 0$ we obtain

$$\begin{aligned} \mathcal{M}_{d5C} &= -\frac{1}{4} \int d\mu (s-k) s^{-1} k^{-1} [s-S]^{-1} [s+k-S-K]^{-1} \\ &\quad \times [S+K-i\tilde{\epsilon}]^{-1} \end{aligned} \quad . \quad (42)$$

Using Eqs. (36), (37), (41) and (42) can show

$$\text{Re} [\mathcal{M}_{d3} + \mathcal{M}_{d4A} + \mathcal{M}_{d5B} + \mathcal{M}_{d5C}] = 0 \quad . \quad (43)$$

IV. CANCELLATION OF REAL GLUON IR DIVERGENCES

For the cross section to order α_s^2 , the amplitudes for the process " $q + \bar{q} \rightarrow \gamma^* + 1 \text{ gluon}$ " as obtained for topological sets e, f, g in Fig. 5 are each to be multiplied by the complex conjugate of the order g amplitude for single gluon emission, etc. In the coherent state approach, this latter order g bremsstrahlung emission amplitude's IR divergences cancel in IR region in eikonal approximation just as in QED. Similarly for " $q + \bar{q} \rightarrow \gamma^* + 2 \text{ gluons}$," the topological set for 2 gluon bremsstrahlung from the quark line to order g^2 is easily shown to be non-divergent in the IR region.

It is also easy to show that the IR divergences in the amplitudes for each of the topological sets in Fig. 5 themselves also cancel in the IR region. Here at most one contour integration is necessary.

For topological set (e), with (a, n, \vec{k}) emitted

$$\begin{aligned}
 \mathcal{M}_{ei} &= \mathcal{M}_{B^t b^t a^t b} \frac{g^3}{(2\pi)^4} \left[\frac{1}{2(2\pi)^3 k_0} \right]^{1/2} \frac{q \cdot e^{(n)}(k)}{q_0} \bar{\mathcal{M}}_{ei} \\
 \bar{\mathcal{M}}_{e0} &= 2\pi \int d^3 \ell \ell^{-2} [L + i\epsilon]^{-1} [k - L - K - i\epsilon]^{-1} \\
 \bar{\mathcal{M}}_{e1} &= -2\pi \int d^3 \ell \ell^{-2} [L + i\epsilon]^{-1} [k - K]^{-1} \\
 \bar{\mathcal{M}}_{e2} &= -2\pi \int d^3 \ell \ell^{-2} [k - K]^{-1} [k - L - K - i\epsilon]^{-1}
 \end{aligned} \tag{44}$$

so the sum of real parts vanishes.

For set (f), (b, ℓ, \vec{k}) emitted

$$\begin{aligned}
\mathcal{M}_{f0} &= -\mathcal{M}_{B^t c^t a} f_{abc} \frac{g^3}{(2\pi)^4} \left[\frac{1}{2(2\pi)^3 k_0} \right]^{\frac{1}{2}} \bar{\mathcal{M}}_{f0} \\
\bar{\mathcal{M}}_{f0} &= -i4\pi \int d^3s \, e(k) \cdot s \, s^{-2} [(\vec{s} + \vec{k})^2]^{-1} \\
&\quad \times [k + S - i\epsilon]^{-1} \\
&= -\bar{\mathcal{M}}_{f1} (\vec{\epsilon} \rightarrow \epsilon)
\end{aligned} \tag{45}$$

For set (h), (a, m, \vec{k}) and (b, n, \vec{s}) emitted,

$$\begin{aligned}
\mathcal{M}_{h0} &= +i\mathcal{M}_{B^t c^t a} f_{abc} g^2 \left[\frac{1}{4(2\pi)^6 s_0 k_0} \right]^{\frac{1}{2}} \\
&\quad \times e(s) \cdot e(k) [-s + k]_0 [(\vec{s} + \vec{k})^2]^{-1} [k + s]^{-1} \\
&= -\mathcal{M}_{h1}
\end{aligned} \tag{46}$$

Set (g) is slightly more complicated because of two energy-orderings. Using notation of (d0) in Fig. 4 but omitting prime so radiated gluon is (b, n, \vec{s}), we express the amplitudes using

$$\begin{aligned}
\mathcal{M}_{gi} &= \mathcal{M}_{B^t c^t a} f_{abc} \frac{g^3}{(2\pi)^4} \left[\frac{1}{2(2\pi)^3 s_0} \right]^{\frac{1}{2}} \bar{\mathcal{M}}_{gi} \\
\int d\lambda &= (2\pi i) \int d^3k e_m^{(n)(s)q_i} \left[\delta_{im} - \frac{k_i k_m}{(\vec{k})^2} \right] \\
&\quad \times (2k)^{-1} [(\vec{s} + \vec{k})^2]^{-1} (q_0)^{-1} .
\end{aligned} \tag{47}$$

For (g0) do k_0 -integration by closing contour below to obtain from gluon propagator

$$\overline{\mathcal{M}}_{g0A} = - \int d\lambda (s+k) [s-k]^{-1} [k+K]^{-1} \quad (48)$$

and from other pole

$$\overline{\mathcal{M}}_{g0B} = 4 \int d\lambda k^{-1} s^{-1} [s-k]^{-1} [s+k]^{-1} [s+K-i\epsilon]^{-1} \quad (49)$$

where the "i ϵ " has been omitted in $[s-k]^{-1}$ since for $s=k$ the term multiplying $[s-k]^{-1}$ vanishes. For (g1) and (g2) we obtain

$$\overline{\mathcal{M}}_{g1} = \int d\lambda (s+k) [k+K]^{-1} [s-k-i\epsilon]^{-1} \quad (50)$$

$$\overline{\mathcal{M}}_{g2} = \int d\lambda (k-s) [k-K]^{-1} [k+s]^{-1} \quad (51)$$

and for (g3), for case \vec{k} emitted,

$$\overline{\mathcal{M}}_{g3A} = - \int d\lambda (s+k) [s-k-i\bar{\epsilon}]^{-1} [s+K-i\bar{\epsilon}]^{-1} \quad (52)$$

and, for \vec{k}' absorbed,

$$\overline{\mathcal{M}}_{g3B} = - \int d\lambda (k-s) [k-K]^{-1} [s+K-i\bar{\epsilon}]^{-1} \quad (53)$$

With these amplitudes we can show

$$\text{Re} [\overline{\mathcal{M}}_{g1} + \overline{\mathcal{M}}_{g2} + \overline{\mathcal{M}}_{g3A} + \overline{\mathcal{M}}_{g3B} + \overline{\mathcal{M}}_{g0A} + \overline{\mathcal{M}}_{g0B}] = 0 \quad (54)$$

ACKNOWLEDGMENT

The author wishes to thank the members of the Fermilab Theory Group, in particular W. Bardeen and C. Quigg, for their hospitality while this work was done. This work was partially supported by the Department of Energy.

APPENDIX: DIAGRAM RULES

Diagram rules for the initial-state are easy to derive using Eqs. (5), (6) and (8), (9). These are similar to the momentum space rules of time-order perturbation theory except the quark and anti-quark lines remain forward in time because there is no fermion-antifermion creation or annihilation. Corresponding to the usual QCD Lagrangian

$$\begin{aligned} \mathcal{L}(x) = & -\frac{1}{4} \left(\partial^\mu A_a^\nu - \partial^\nu A_a^\mu - gf_{abc} A_b^\mu A_c^\nu \right)^2 \\ & - \bar{\psi} \left[\gamma_\mu \left(-i \partial^\mu + g t_a A_a^\mu \right) + m \right] \psi \\ & + \dots \end{aligned} \quad , \quad (A1)$$

the vertices needed in the text are:

(i) gluon (a, m, \vec{k}) attached to incident quark, p,

$$\frac{g \, p \cdot e^{(m)}}{[2(2\pi)^3 k_0]^{1/2} p_0} (t_a) \quad (A2)$$

with $(t_a) \rightarrow (-t_a^T)$ for gluon attached to incident antiquark. The energy denominator $[i(E_0 - E_n - i\epsilon)]^{-1}$ for n-th intermediate state is obtained by working outward, to

right, from broken line separating graph from initial-state with, E_0 = energy of state at broken line, and, E_n = energy of n-th intermediate state. For gluon of momentum \vec{k}

$$[i(E_0 - E_1 - i\epsilon)]^{-1} = \left[i \left(\mp \frac{\vec{k} \cdot \vec{p}}{p_0} - i\epsilon \right) \right]^{-1}$$

respectively for \vec{k} absorbed, emitted. At each vertex three-momentum is conserved, and the quarks and gluons are on-mass-shell. There is an overall factor $(i)^n$ for each state part where n is order of state part.

(ii) gluon (a, ℓ , \vec{k}) created, and gluons (b, m, $\vec{\ell}$) and (c, n, \vec{m}) annihilated

$$\frac{i g f_{abc}}{(2\pi)^{3/2} [8k_0 \ell_0 m_0]^{1/2}} V_{\mu\nu\eta} (\pm k, \mp \ell, \mp m) e_{\mu}^{(\ell)(k)} e_{\nu}^{(m)(\ell)} e_{\eta}^{(n)(m)} \quad (A3)$$

with lower signs for (c, n, \vec{m}), (b, m, $\vec{\ell}$) created and (a, ℓ , \vec{k}) annihilated. All three-momentums point to left.

(iii) for gluons (a, ℓ , \vec{k}), (b, m, $\vec{\ell}$), (c, n, \vec{n}) annihilated

$$\frac{i g f_{abc}}{(2\pi)^{3/2} [8k_0 \ell_0 n_0]^{1/2}} V_{\mu\nu\eta} (\mp k, \mp \ell, \mp n) e_{\mu}^{(\ell)(k)} e_{\nu}^{(m)(\ell)} e_{\eta}^{(n)(n)} \quad (A4)$$

with lower signs for creation.

In (ii) and (iii),

$$V_{\mu\nu\eta}(k, q, r) = [g_{\mu\nu}(k - q)_{\eta} + g_{\nu\eta}(q - r)_{\mu} + g_{\mu\eta}(r - k)_{\nu}]$$

and energy denominators are

$$[i(E_0 - E_1 - i\epsilon)]^{-1} = [i(\pm k_0 \mp \ell_0 \mp m_0 - i\epsilon)]^{-1} , \quad [i(\mp k_0 \mp \ell_0 \mp n_0 - i\epsilon)]^{-1}$$

respectively.

Rule for quartic vertex is not needed here, but it can be read off of Eq. (14) in Ref. 8.

For Coulomb gauge used in text, "effective vertices" are needed since in time-ordered perturbation theory Coulomb gluons contribute via an "instantaneous interaction." We find:

(a) Coulomb exchange between fermions:

$$t_c t_c \left[\frac{-i g^2}{(2\pi)^3} \right] \frac{1}{(\vec{k})^2} \quad (A5)$$

for \vec{p} and \vec{q} quarks with Coulomb gluon, \vec{k} , from fermion q to p with $[i(k \cdot q/q_0 - k \cdot p/p_0 - i\epsilon)]^{-1}$. This is order g^2 effective coupling, so if alone in state it has "(i)² divided by energy denominator" as its coefficient. Here and below, substitute $(t_c) \rightarrow (-t_c^T)$ for antiquark.

(b) For "Y type" radiation by fermion:

$$t_a \left[\frac{g^2 f_{abc}}{(2\pi)^3 [4 \ell_0 m_0]^{1/2}} (\mp \ell \pm m)_0 \vec{e}^{(m)}(\ell) \cdot \vec{e}^{(n)}(m) \right] \frac{1}{(\vec{r})^2} \quad (A6)$$

for Coulomb gluon, \vec{r} from fermion p , in which \vec{r} creates [annihilates] transverse gluons (c, n, \vec{m}) , $(b, m, \vec{\ell})$, with energy denominators respectively

$$\left[i \left(-|\vec{r}| \pm \ell_0 \pm m_0 + \frac{r \cdot p}{p_0} - i\epsilon \right) \right]^{-1} , \quad \vec{r} = \pm(\vec{m} + \vec{\ell})$$

and

$$t_c \left[\frac{-g^2 f_{abc}}{(2\pi)^3 [4k_0 \ell_0]^{1/2}} (k + \ell)_0 \vec{e}^{(\ell)}_{(k)} \cdot \vec{e}^{(n)}_{(\ell)} \right] \frac{1}{(\vec{r})^2} \quad (A7)$$

for transverse (a, ℓ, \vec{k}) created and $(b, m, \vec{\ell})$ annihilated with $\left[i(k_0 - \ell_0 - |\vec{r}| + \frac{\vec{r} \cdot \vec{p}}{p_0} - i\epsilon) \right]^{-1}$ and $\vec{r} = \vec{k} - \vec{\ell}$.

(c) For gluon radiated by Coulomb gluon exchanged between fermions:

$$t_c t_b \left[\frac{-i g^3 f_{abc}}{(2\pi)^{9/2} [2k_0]^{1/2}} (\vec{n} - \vec{r}) \cdot \vec{e}^{(\ell)}_{(k)} \right] \frac{1}{(\vec{r})^2 (\vec{n})^2} \quad (A8)$$

for Coulomb gluons, \vec{r} from q , \vec{n} from p , with transverse (a, ℓ, \vec{k}) created [annihilated] and $\left[i(k_0 - |\vec{r}| + \frac{\vec{r} \cdot \vec{p}}{p_0} - |\vec{n}| + \frac{\vec{n} \cdot \vec{p}}{p_0} - i\epsilon) \right]^{-1}$ and $\vec{k} = \pm(\vec{r} + \vec{n})$.

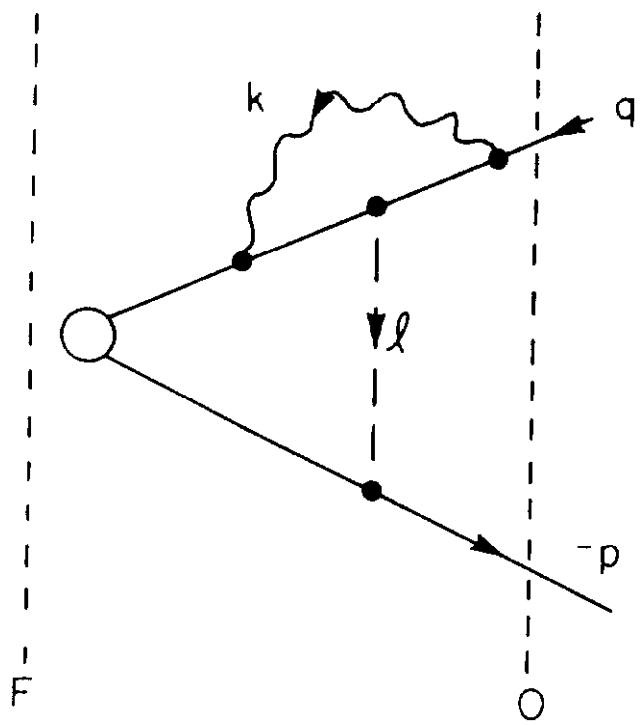
Diagram rules for non-trivial final-state parts, including diagrams in which gluons directly connect initial-state and final-state (i.e. graph part is a "disconnected graph" as in some diagrams in Ref. 8), similarly follow from Eqs. (5) and (7), $\langle \psi_{as} | = \lim_{t' \rightarrow \infty} (\langle \psi_F | Z(t'))$, and Eqs. (8) and (9).

REFERENCES

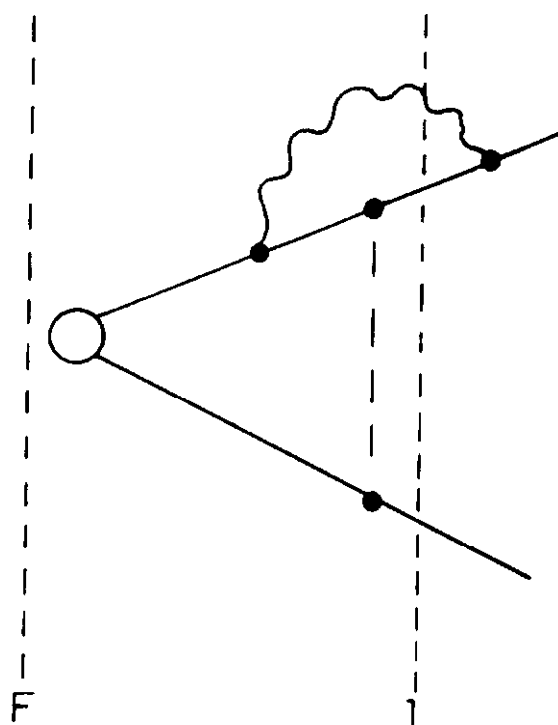
- ¹ R. Doria, J. Frenkel and J.C. Taylor, Nucl. Phys. B168 (1980) 93.
- ² F. Bloch and A. Nordsieck, Phys. Rev. 52 (1937) 54; D.R. Yennie, S.C. Frautschi, and H. Suura, Ann. Phys. (N.Y.) 13 (1961) 379.
- ³ A. Andrasi, M. Day, R. Doria, J. Frenkel, and J.C. Taylor, Oxford University preprint No. 37/80 (1980); A. Andrasi, M. Day, R. Doria, J.C. Taylor, C. Carneiro, J. Frenkel, and M. Thomaz, Oxford University-Universidade de Sao Paulo preprint (1980).
- ⁴ C. Di'Lieto, S. Gendron, I.G. Halliday, C.T. Sachrajda, Imperial College-Southampton University preprint ICTP/79-80/47, SHEP 79/80-6 (1980).
- ⁵ S.V. Libby and G. Sterman, Phys. Rev. D19 (1979) 2468.
- ⁶ T. Kinoshita, J. Math. Phys. 3 (1962) 650; T.D. Lee and M. Nauenberg, Phys. Rev. 133 (1964) 1549.
- ⁷ D.R. Butler and C.A. Nelson, Phys. Rev. D18 (1978) 1196; C.A. Nelson, in Proceedings of Neutrino Physics Conference, Purdue University, Lafayette, Indian (1978).
- ⁸ C.A. Nelson, Fermilab-Pub-80/59-THY (July 1980).
- ⁹ P.P. Kulish and L.D. Faddeev, Teor. Mat. Fiz. 4 (1970) 153 [Theor. Math. Phys. 4 (1970) 745], and see J. Dollard, J. Math. Phys. 5 (1964) 729.
- ¹⁰ V. Chung, Phys. Rev. 140 (1965) B1110; and T.W. B. Kibble, *ibid.* 173 (1968) 1527; 174 (1968) 1882; 175 (1968) 1624; D. Zwanziger, Phys. Rev. Lett. 30 (1973) 934; Phys. Rev. D7 (1973) 1082; D11 (1975) 3481; D11 (1975) 3504; S.S. Schweber, Phys. Rev. D7 (1973) 3114; N. Papanicolaou, Ann. Phys. (N.Y.) 89 (1975) 423; and F. Rohrlich, Phys. Rev. D12 (1975) 1832. See also J.L. Gervais and D. Zwanziger, CERN preprint TH-2861 (1980).
- ¹¹ J. von Neumann, Comp. Mat. 6 (1938) 1.

FIGURE CAPTIONS

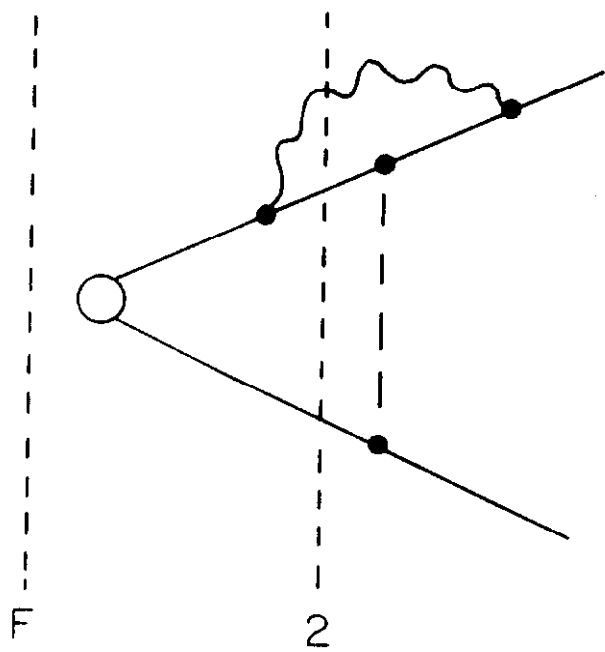
- Fig. 1: Figures 1 thru 4 are the distinct topological sets of diagrams which contribute to N in Eq. (11) to order α_s^2 for the process " $q + \bar{q} \rightarrow \gamma^*$." Cancellation of IR divergences is found to occur separately for each topological set. The open circles denote the emission of the hard virtual photon. The Coulomb gluon propagator is represented by a broken line, the transverse gluon propagator by a wavy line. On-shell particles bridge the initial-state, graph, and final-state parts. The two vertical broken lines, with small dashes, display the separation of each diagram into these three parts. Fig. 1 is the non-Abelian topological set, (a).
- Fig. 2: Diagrams in topological set (b) with the 3-gluon vertex and with transverse gluon emission occurring first on the incident quark line.
- Fig. 3: Diagrams in topological set (c) with the 3-gluon vertex and with transverse gluon absorption occurring second on the incident quark line.
- Fig. 4: Diagrams in topological set (d) with the 3-gluon vertex and with two transverse gluons attached to the incident quark line.
- Fig. 5: Topological sets of gluon emission diagrams which contribute to N in Eq. (11) to order α_s^2 for the process " $q + \bar{q} \rightarrow \gamma^* + 1$ soft gluon" [sets e, f, g] and for " $q + \bar{q} \rightarrow \gamma^* + 2$ soft gluons" [set h].



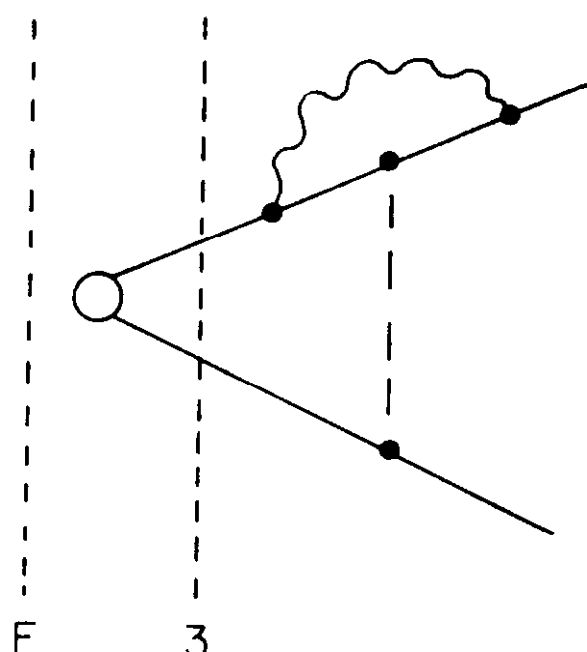
(a0)



(a1)



(a2)



(a3)

Figure 1

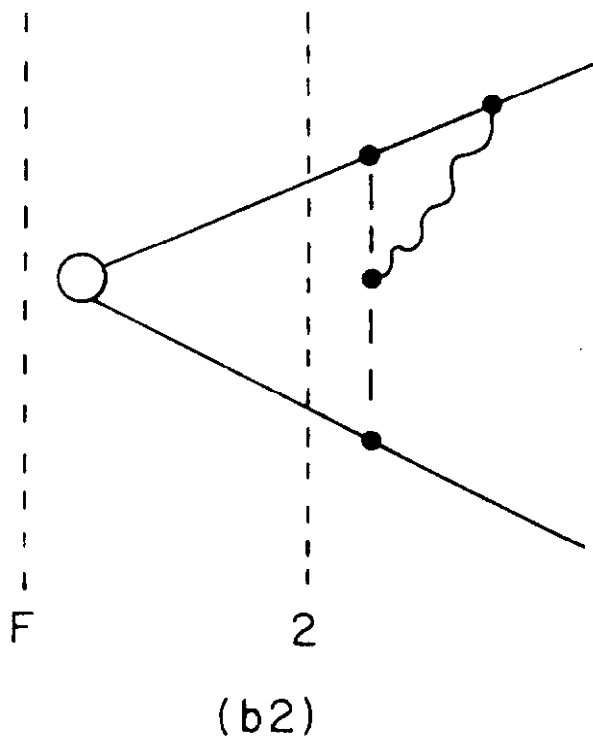
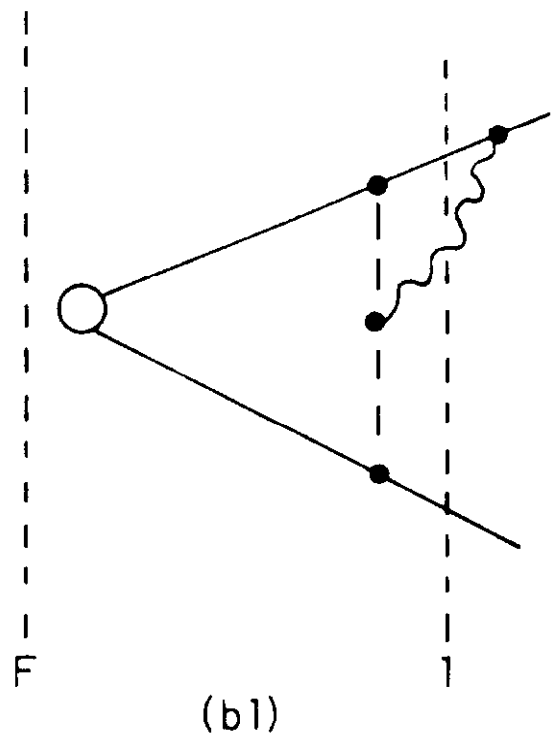
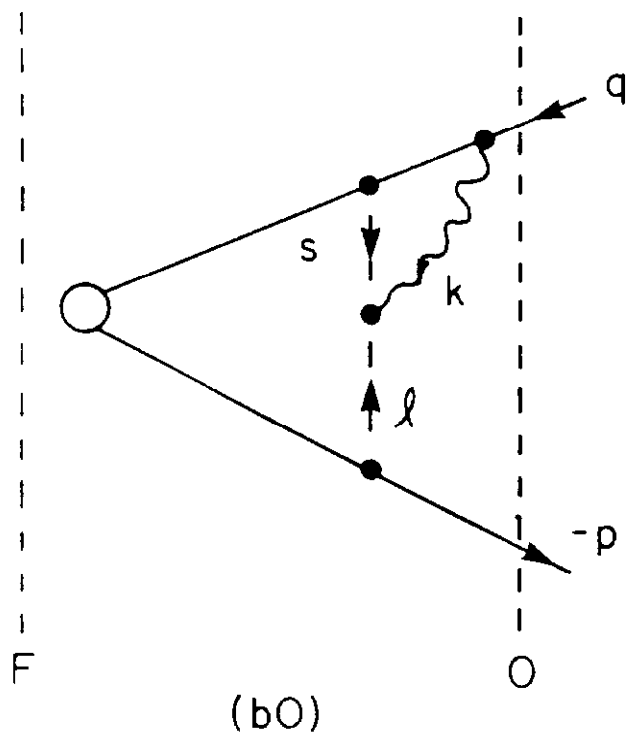
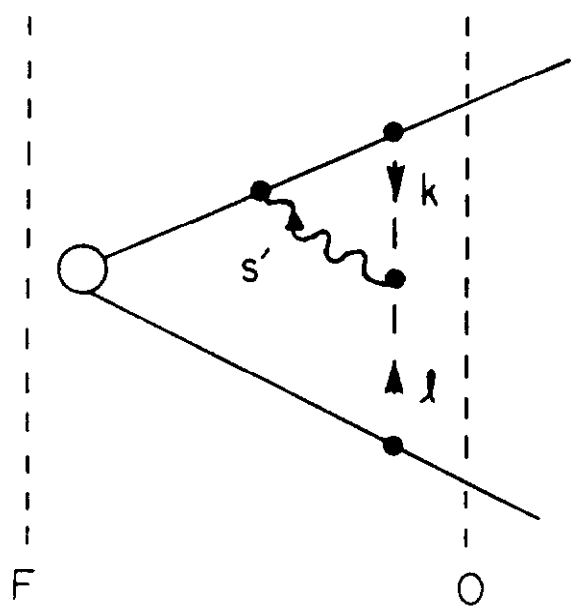
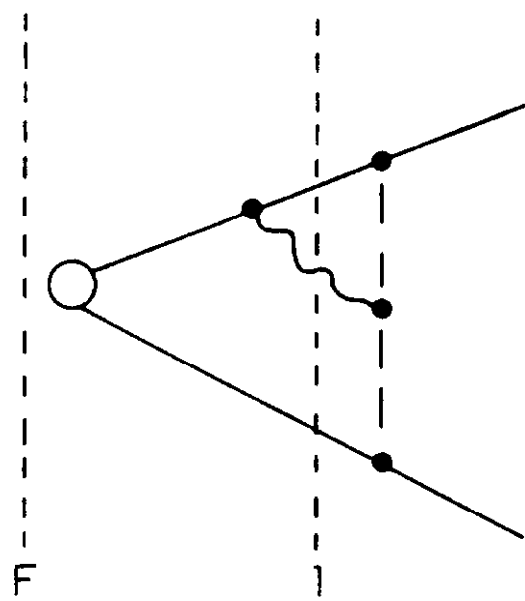


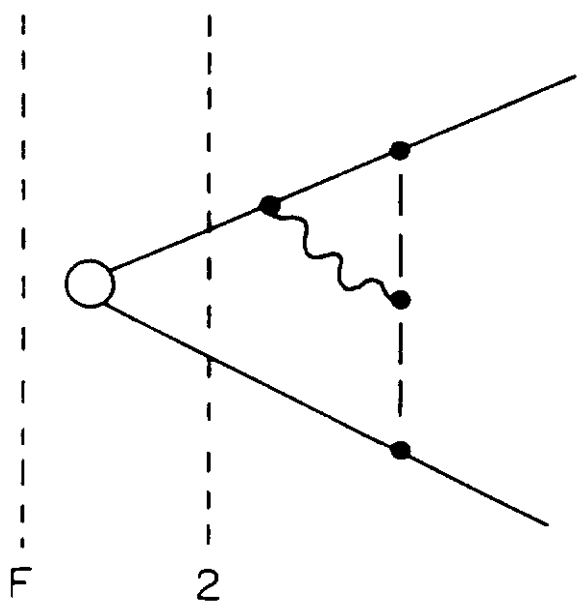
Figure 2



(c0)



(c1)



(c2)

Figure 3

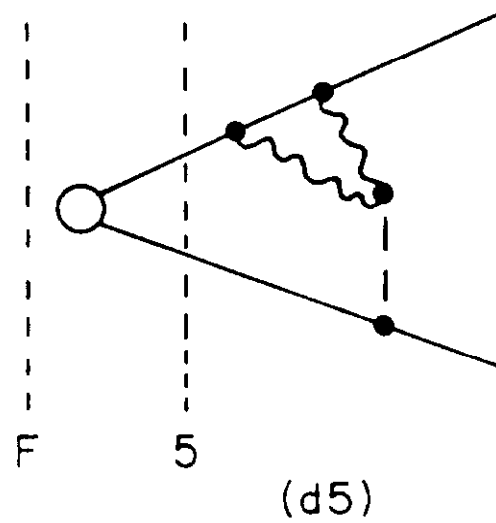
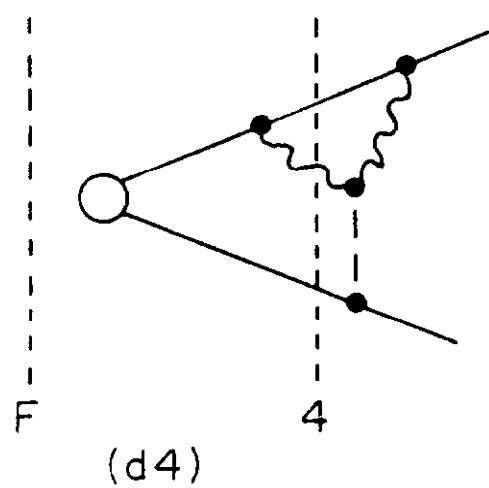
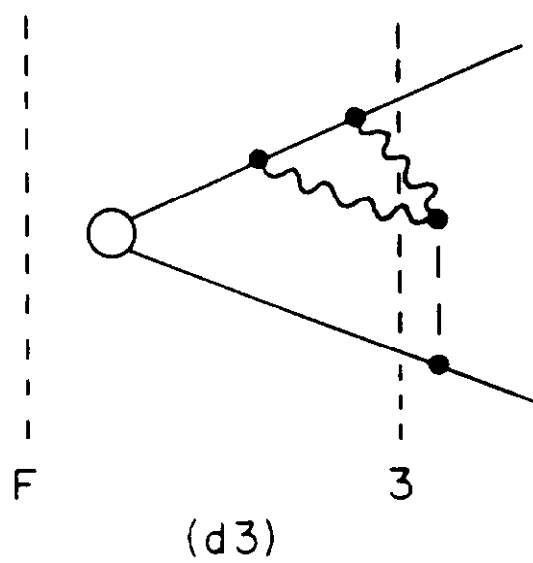
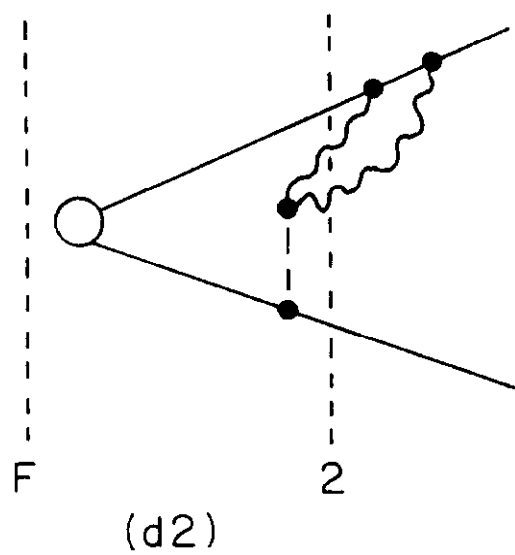
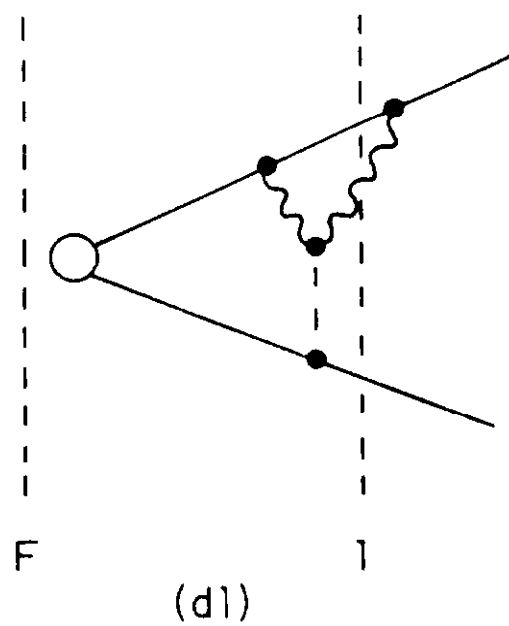
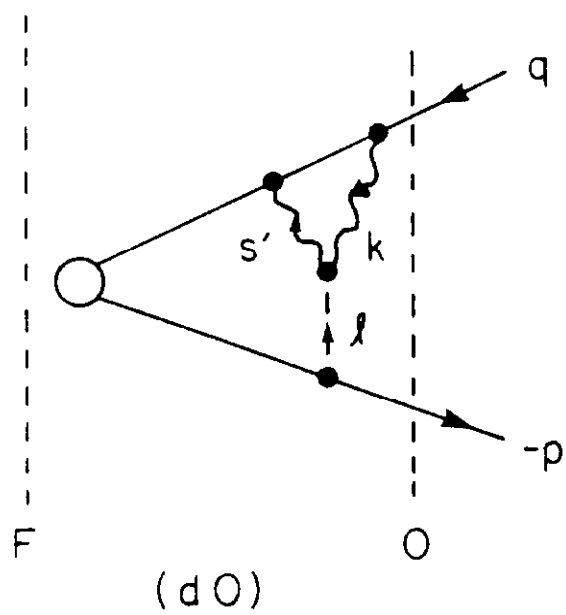


Figure 4

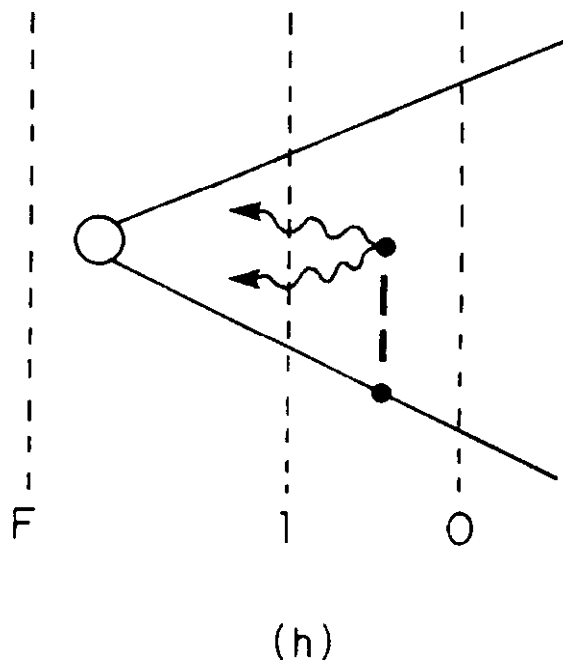
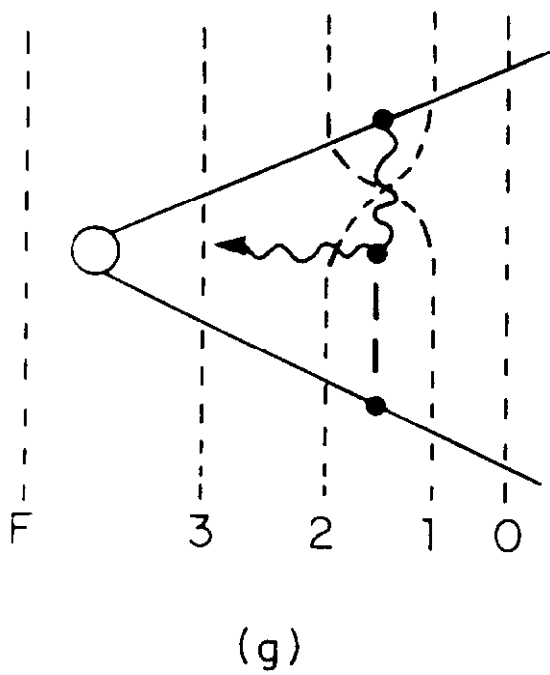
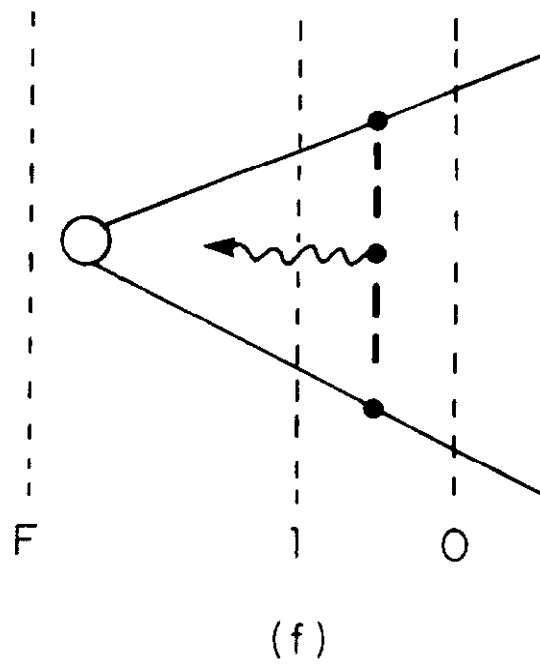
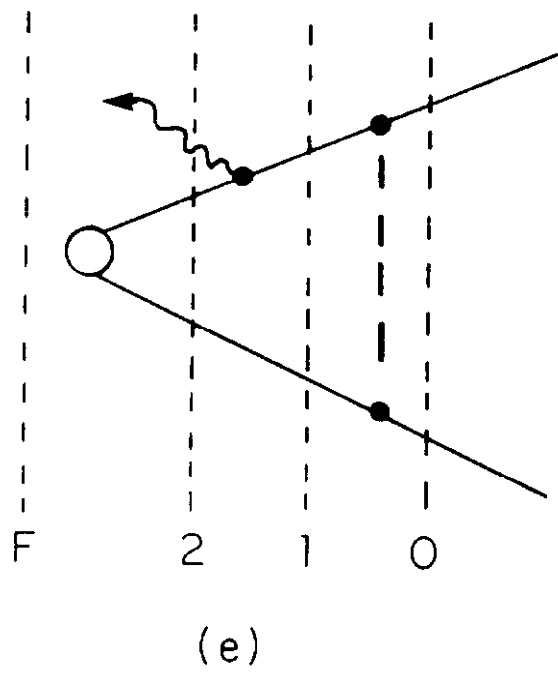


Figure 5